

Assessment of the reliability of popular satellite products in characterizing the water balance of the Yangtze River Basin, China

Dan Zhang, Qi Zhang, Adrian D. Werner and Renying Gu

ABSTRACT

This study investigates the water balance of the Yangtze River Basin (YRB) during 2003–2012 using the Tropical Rainfall Measuring Mission precipitation, the Moderate Resolution Imaging Spectroradiometer evapotranspiration and the Gravity Recovery and Climate Experiment total water storage change. The bias, absolute error and correlation coefficient are used to quantify water balance performances at monthly and annual time steps. The results show that the absolute error in the YRB water balance was 18.1 mm/month and 152.5 mm/yr at monthly and annual time steps accounting for 20% and 14% of YRB precipitation, respectively. The three satellite products were combined through a water balance equation to estimate monthly and annual stream flow, which was in error by 19.4 mm/month and 76.7 mm/yr, accounting for 22% and 7% of YRB precipitation, respectively. Trends in YRB water balance components at annual time steps obtained from satellite products were in the range 83–318% of the corresponding trends from alternative datasets (e.g., ground-based measurements, land-surface modelling, etc.), which performed significantly better than monthly time series. The results indicate that the YRB water balance can be evaluated using multiple satellite products to a reasonable accuracy at annual time steps.

Key words | multiple satellite products, water balance changes, water balance closure, Yangtze River Basin

Dan Zhang

Qi Zhang (corresponding author)
Key Laboratory of Watershed Geographic Sciences,
Nanjing Institute of Geography and Limnology,
Chinese Academy of Sciences,
Nanjing,
China
E-mail: Qzhang@niglas.ac.cn

Dan Zhang

State Key Laboratory of Hydrology-Water
Resources and Hydraulic Engineering,
Hohai University,
Nanjing,
China

Adrian D. Werner

National Centre for Groundwater Research and
Training, and School of the Environment,
Flinders University,
Adelaide,
Australia

Renying Gu

Ningbo Yinzhou Meteorological Bureau,
No. 1858 South Tiantong Road,
Ningbo,
China

INTRODUCTION

Basin-scale water balance assessment is often subdivided into the following components: precipitation, evapotranspiration, river discharge and total water storage change (TWSC) (Maidment 1992), where TWSC represents changes in the water stored in both surface and subsurface domains. The evaluation of water balance components and their temporal trends is an essential requirement of water resources investigations of

river and lake basins, in particular, for the development of effective management strategies for water and ecosystem services (Wilson *et al.* 2001). Land-based measurements of these variables are restricted by several factors, such as the sparseness of meteorological and hydrological stations for precipitation and evapotranspiration observation, and the spatial heterogeneities inherent in natural systems (Pohl & van Genderen 1998; Lakshmi *et al.* 2011; Adjei *et al.* 2014). Further, recording instruments are usually situated in flat areas, and hence regions of steep topography are typically under-represented (Swenson & Wahr 2009). The application of satellite-based methods provides advantages of improved spatial coverage, including for mountainous areas that are

This is an Open Access article distributed under the terms of the Creative Commons Attribution Licence (CC BY-NC-ND 4.0), which permits copying and redistribution for non-commercial purposes with no derivatives, provided the original work is properly cited (<http://creativecommons.org/licenses/by-nc-nd/4.0/>).

doi: 10.2166/nh.2016.138

otherwise difficult to access (e.g., Benz *et al.* 2004; Sheffield *et al.* 2009; Finsen *et al.* 2014; Wu *et al.* 2015).

The most popular methods for whole-of-catchment water balance studies are often based on satellite products, such as the Tropical Rainfall Measuring Mission (TRMM), the Moderate Resolution Imaging Spectroradiometer (MODIS) and the Gravity Recovery and Climate Experiment (GRACE) (e.g., Armanios & Fisher 2014; Oliveira *et al.* 2014). The largest component requiring quantification in any catchment is precipitation. Accurate precipitation estimates are critical for reliable water balance evaluations (Al-Mukhtar *et al.* 2014; Kang & Merwade 2014). TRMM is a research satellite designed to improve the characterization of precipitation distribution across large areas (Kummerow *et al.* 1998; Huffman *et al.* 2007; Castro *et al.* 2015; Xu *et al.* 2015). Products from TRMM are the most popular and widely used precipitation datasets for application to basin hydrological analysis (e.g., Li *et al.* 2012, 2014; Yang & Nesbitt 2014). In general, the performance of TRMM precipitation at annual and monthly time steps is very good, whereas higher frequency datasets are less reliable (e.g., Barros *et al.* 2000; Wolff *et al.* 2005; Su *et al.* 2008; Armanios & Fisher 2014; Zhao *et al.* 2015).

The second-largest component of any catchment water balance is typically the evapotranspiration. The MODIS global terrestrial evapotranspiration dataset (MOD16), established by Mu *et al.* (2011), is widely used in the evaluation of regional water and energy balances (e.g., Sun *et al.* 2007; Venturini *et al.* 2008; Kim *et al.* 2012; Wang & Dickinson 2012; Corbari *et al.* 2014). For example, Kim *et al.* (2012) validated the performance of MOD16 in Asia and concluded that it can estimate actual evapotranspiration with reasonable accuracy at monthly time scales. He & Shao (2014) compared MODIS evapotranspiration with actual evapotranspiration from a water balance method, and found a reasonable match for China at annual time steps (i.e., correlation coefficient r of 0.91).

Perhaps the most difficult component of a basin water balance to quantify from field measurements is TWSC. In March 2002, NASA launched GRACE satellites to measure earth's gravitational field with enough precision to infer variations in terrestrial water mass over large regions (Rodell *et al.* 2004; Tapley *et al.* 2004). Relative to conventional *in situ* observations and other remote sensing methods, GRACE products derive integrated information on TWSC in terms of all surface and subsurface water components (Landerer & Swenson 2012).

GRACE data are thought to provide a reasonable estimation of TWSC (Moiwo *et al.* 2013; Long *et al.* 2014), and have been used in a variety of hydrological studies, ranging from river basins to continental and even global estimates (e.g., Reager & Famiglietti 2013; Tang *et al.* 2014; Wang *et al.* 2014a).

A number of previous basin water balance studies have relied on multiple satellite products (e.g., Sahoo *et al.* 2011; Armanios & Fisher 2014; Oliveira *et al.* 2014; Wang *et al.* 2014a). For example, Sahoo *et al.* (2011) assessed the water budgets of ten large river basins from across the globe using 2003–2006 data from nine satellite products. They found that errors in precipitation were the main source of non-closure of basin water balances. Armanios & Fisher (2014) used the same three products as adopted in the current study (i.e., TRMM, MODIS and GRACE) to investigate the water budget of Tanzania. They concluded that only the long-term (i.e., 2003–2010) water balance could be evaluated using these products. Oliveira *et al.* (2014) estimated stream flow for the Brazilian savanna by applying TRMM, MODIS and GRACE data in water balance calculations, and the results were used to detect hydrological drought. However, the accuracy of estimated stream flow was not validated by observed stream flow. Moreover, there is a need to explore the discrepancy between hydrological trends obtained from TRMM, MODIS and GRACE data, relative to ground-based/model-based datasets, given that previous studies have explored the accuracy of these satellite products using comparisons of absolute values only.

The current study uses TRMM, MODIS and GRACE to study the water balance of the Yangtze River Basin (YRB), China. Under the impact of changing climate and human activities, the YRB has experienced a high frequency of extreme hydrological events (i.e. droughts and floods) over the last few decades (e.g., Dai *et al.* 2008; Huang *et al.* 2014; Zhang *et al.* 2014). Previous studies of the YRB have mainly focused on the flow and water level trends of surface water systems, while subsurface water storage changes have received little consideration. In addition, the construction of the Three Gorges Dam (TGD), the largest hydroelectric power station in the world, has significantly modified some of the hydrological components of the YRB (Zhang *et al.* 2014). However, a comprehensive investigation of the YRB water balance and its temporal trends has not been undertaken, and yet these are critical for YRB water resource management, water project planning and ecosystem protection.

The current study aims to: (i) explore the accuracies of TRMM precipitation, MODIS evapotranspiration and GRACE TWSC based on the data of ground-based measurements and land surface models of the hydrology of the YRB during 2003–2012; (ii) characterize the water balance closure associated with the application of multiple remote sensing products; and (iii) evaluate changes in the YRB water balance during 2003–2012. The results are expected to provide an assessment of the reliability of popular satellite products in undertaking a water balance characterization at the scale of the YRB. The current study also extends previous satellite-based water balance investigations by examining the uncertainty in trends that are obtained by comparing to field-based datasets and model-based datasets.

STUDY AREA

The Yangtze River (24–35° N, 90–122° E), originating from the Qinghai-Tibetan Plateau, flows from west to east and then discharges to the East China Sea. The YRB experiences subtropical and temperate climates, with a mean temperature of 14 °C, and average annual precipitation of about 1,100 mm, of which 76% occurs during April to September

(based on meteorological observations during 1960–2010). The average stream flow is about $9.5 \times 10^{11} \text{ m}^3/\text{yr}$, which accounts for 35% of China's total (Varis & Vakkilainen 2001). The basin-averaged runoff coefficient, i.e., ratio of average stream flow to average precipitation (multiplied by catchment area), is approximately 0.5.

For the purposes of the current study, the YRB is subdivided into three main sub-basins, referred to here as the upper reaches (upstream of Yichang station; Figure 1), the middle reaches (between Yichang and Datong stations; Figure 1) and the lower reaches (downstream of Datong station). Yichang and Datong are two major hydrological stations for the YRB, and Datong station is the last hydrological station which has stream flow observations for the entire upstream catchment of the YRB. Only the upper and middle reaches were considered in the current analysis. The TGD is about 44 km upstream of Yichang station (Guo *et al.* 2012; Lai *et al.* 2014). The upper reaches of the YRB has a drainage area of approximately $1.0 \times 10^6 \text{ km}^2$, and the middle reaches of the YRB has a drainage area of approximately $0.7 \times 10^6 \text{ km}^2$. The lower reaches of the YRB is flat, creating a complex river network lacking in flow gauging stations, and as such, water balance analysis was not undertaken for this part of the YRB.

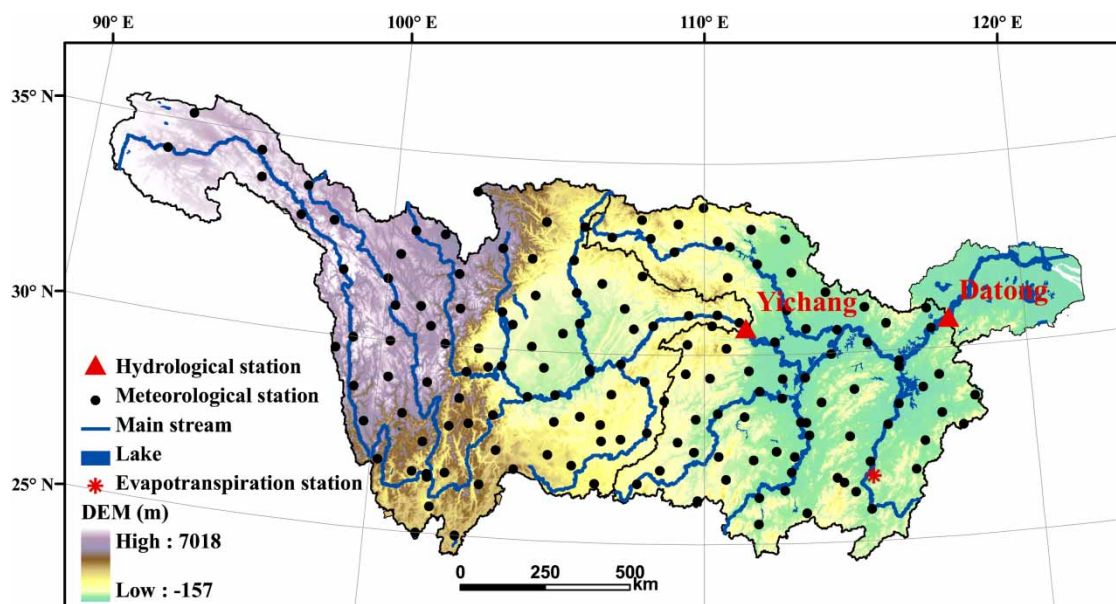


Figure 1 | YRB showing topography and ground-based measurement sites.

DATA AND METHODS

Satellite products

Three satellite products were employed in this study (Table 1), including precipitation from TRMM 3B43 Version 7, evapotranspiration from MODIS MOD16, and TWS from GRACE, using observations from the period January 2003 to December 2012.

The TRMM precipitation product (P_{TRMM} , mm/month) is a combination of 3-hourly merged high-quality infrared estimates and the latest spatial distributions of gauged precipitation from the Global Precipitation Climatology Center (Huffman *et al.* 2007). There were several important changes in Version 7 of the TRMM series of data products, such as additional output fields, uniformly reprocessed input data using current algorithms, and a new infrared brightness temperature dataset. The TRMM dataset covers the latitude band 50°N-S (Huffman *et al.* 2007). The spatial resolution of TRMM is 0.25° (approximately 25 km) and the temporal resolution is monthly.

The MODIS global terrestrial evapotranspiration product (ET_{MODIS} , mm/month) was updated based on a new algorithm by Mu *et al.* (2011), including vegetation cover fraction, daytime and night time evapotranspiration, soil heat flux, wet surface

fraction and evaporation from wet canopy surfaces. The spatial resolution of MODIS is 1 km and the temporal resolution is monthly. Evapotranspiration from four land surface models (Noah model, VIC model, MOSIC model and CLM model) of the Global Land Data Assimilation System (GLDAS) was employed to compare with the MODIS data, in a similar manner to previous evapotranspiration studies by Reichle *et al.* (2004), Peters-Lidard *et al.* (2011) and Cai *et al.* (2014).

The Release-05 GRACE data provided by the Geo-ForschungsZentrum Potsdam were employed in this study. Since GRACE observations tend to be attenuated during sampling and post-processing at small spatial scales, the true signal amplitude was adjusted by the scaling factors based on the Community Land Model V4.0 (Landerer & Swenson 2012). The spatial resolution of GRACE TWS is 1° (approximately 110 km) and the temporal resolution is monthly.

Ground-based observations

Precipitation data (P_{OBS} , mm/month) in the form of monthly totals from 160 meteorological stations in the YRB were provided by the National Climatic Centre of China Meteorological Administration for the period 2003–2012.

Table 1 | Datasets used in this study

Data	Elements	Source	Resolution/ station numbers	Period	Reference	Download site
Grid products	Precipitation	TRMM 3B43 V7	0.25° × 0.25°	2003–2012	Huffman <i>et al.</i> (2007)	http://disc.sci.gsfc.nasa.gov/
	Evapotranspiration	MODIS MOD16	1 km × 1 km	2003–2012	Mu <i>et al.</i> (2011)	http://www.ntsg.umd.edu/ project/et
		GLDAS_NOAH	0.25° × 0.25°	2003–2012	Houser <i>et al.</i> (2001)	http://disc.sci.gsfc.nasa.gov/ services/grads-gds/gldas/ index.shtml
		GLDAS_VIC	1° × 1°	2003–2012		
		GLDAS_CLM	1° × 1°	2003–2012		
	GLDAS_MOS	1° × 1°	2003–2012			
Total water storage	GRACE	1° × 1°	2003–2012	Landerer & Swenson (2012)	http://www.csr.utexas.edu/ grace/	
Ground- based data	Precipitation	Meteorological station	160 stations	2003–2012	–	China Meteorological Bureau
	Evapotranspiration	FLUX station	1 station	2003–2004	–	http://www.chinaflux.org/ index/index.asp
	Stream flow	Hydrological station	2 station	2003–2012	–	Yangtze River Hydrological Bureau, China

These were used to test the accuracy of TRMM precipitation. The only evapotranspiration observation station, Qianyanzhou, is located in the southeast of the YRB (Figure 1). Daily evapotranspiration data, based on the eddy covariance method, were summed to monthly totals (ET_{OBS} , mm/month) from the observation record of 1st January 2003 to 31st December 2004. ET_{OBS} was compared to ET_{MODIS} and GLDAS evapotranspiration (at the grid containing Qianyanzhou station).

Daily stream flow records from Yichang and Datong hydrological stations were obtained from the Yangtze River Hydrological Bureau of China for 2003–2012. The runoff into the middle reaches of the YRB was considered as the difference in stream flow at Datong and Yichang stations. Records of daily stream flow were summed to monthly totals and converted to specific discharge (Q_{OBS} , mm/month) by dividing by the respective basin areas. The locations of meteorological and hydrological stations are shown in Figure 1.

Water balance analysis for the YRB

The water balance analysis of this study equates water storage changes to the sum of water fluxes entering and leaving a particular region, for the purposes of evaluating basin-scale water balance trends. That is, TWSC is compared to the residual of incoming precipitation, outgoing evapotranspiration and stream discharge (i.e., groundwater discharge into and out of the region of interest is neglected), which can be expressed as:

$$P - ET - Q = \Delta S \quad (1)$$

where P is precipitation (mm/month); ET is evapotranspiration (mm/month); Q is stream discharge (mm/month); ΔS is TWSC (mm/month).

TWSC can be determined from GRACE measurements (ΔS_{GRACE}), expressed as the difference between GRACE total water storage (TWS) for two consecutive months (Long *et al.* 2014):

$$\Delta S_{GRACE}(t) = TWS(t) - TWS(t - 1) \quad (2)$$

The GRACE TWS signal exhibited significant noise, and so a temporal three-point average window for the TWS time

series, in a similar manner to Wang *et al.* (2014b), was used in the current study.

The error in the implementation of Equation (1) using remotely sensed data is explored by comparing the left side components with ΔS_{GRACE} . That is, the difference in water balance components on the left side of Equation (1) is firstly calculated by substituting P_{TRMM} , ET_{MODIS} and Q_{OBS} for the respective Equation (1) variables, to obtain the residual $\Delta S_{WB}(t)$ of water balance fluxes. Then, the water balance error $\varepsilon(t)$ (mm/month) is estimated as the difference between this and the GRACE-based TWSC, as

$$\varepsilon(t) = \Delta S_{GRACE}(t) - (P_{TRMM}(t) - ET_{MODIS}(t) - Q_{OBS}(t)) \quad (3a)$$

simplified as

$$\varepsilon(t) = \Delta S_{GRACE}(t) - \Delta S_{WB}(t) \quad (3b)$$

The average absolute error ($\bar{\varepsilon}$, mm/month) for a given period of n months is calculated as

$$\bar{\varepsilon} = \frac{1}{n} \sum_{t=1}^n |\varepsilon(t)| \quad (4)$$

The bias ($\bar{\varepsilon}_b$, mm/month) is simply the time-averaged error:

$$\bar{\varepsilon}_b = \frac{1}{n} \sum_{t=1}^n \varepsilon(t) \quad (5)$$

Bias offers insight into over- and underestimation relative to alternative methods. The average P_{TRMM} error ($\bar{\varepsilon}_{TRMM}$, mm/month) and bias ($\bar{\varepsilon}_{TRMM,b}$, mm/month) are estimated by Equations (4) and (5), except using the difference between P_{TRMM} and P_{OBS} as the error time series. The average ET_{MODIS} error ($\bar{\varepsilon}_{MODIS}$, mm/month) and bias ($\bar{\varepsilon}_{MODIS,b}$, mm/month) are estimated in a similar manner, i.e. using Equations (4) and (5) and the difference between ET_{MODIS} and GLDAS evapotranspiration. The error in GRACE TWSC ($\bar{\varepsilon}_{GRACE}$, mm/month) is estimated by the GRACE measurement error and leakage error (Landerer & Swenson 2012), which is provided with the GRACE TWS data.

Equation (1) can be modified to make stream flow the dependent variable, allowing for an estimate of the spatial distribution in stream discharge Q_{RS} (mm/month) for the YRB based on P_{TRMM} , ET_{MODIS} and ΔS_{GRACE} . The resolution of Q_{RS} is 1° (the coarsest resolution among the three products). Then, the error in Q_{RS} , $\bar{\epsilon}_Q$ (mm/month), can be estimated as:

$$\bar{\epsilon}_Q = (\bar{\epsilon}_{TRMM}^2 + \bar{\epsilon}_{MODIS}^2 + \bar{\epsilon}_{GRACE}^2)^{0.5} \quad (6)$$

The error in Q_{RS} is also estimated by Equations (4) and (5), except using the difference between Q_{RS} and Q_{OBS} as the error time series, expressed as $\bar{\epsilon}_{Q2}$. Correlation coefficient r is used to analyze the errors in water balance components and their trends. Trends in water balance components are estimated using linear regression, and the T-test (Sun *et al.* 2014) is conducted to determine whether trends are significant at 95% ($P < 0.05$) and 90% ($P < 0.1$) confidence levels.

RESULTS AND DISCUSSION

Accuracy of TRMM, MODIS and GRACE water balance components

The accuracy of P_{TRMM} was evaluated by comparison with the time series of P_{OBS} from 160 meteorological stations in

the YRB. Figure 2 shows that the resulting value of r for the match between P_{TRMM} and P_{OBS} was greater than 0.9 at 67% of stations, which indicates that P_{TRMM} reproduces reasonably well P_{OBS} across over 2/3 of the YRB. $\bar{\epsilon}_{TRMM}$ was lower than 10 mm/month at 74% of stations. As given in Figure 3, the YRB $\bar{\epsilon}_{TRMM,b}$ value of 4.4 mm/month indicates that TRMM over-estimated ground-based precipitation. At annual time steps, $\bar{\epsilon}_{TRMM}$ was 54.3 mm/yr for the YRB (shown in Table 2), accounting for 5% of the corresponding P_{OBS} . $\bar{\epsilon}_{TRMM}$ in the middle reaches of the YRB was larger than that in the upper reaches of the YRB at both monthly and annual steps. Scheel *et al.* (2011) reported that precipitation is higher in the lower latitude and altitude areas (e.g., the monthly P_{OBS} averages 72.8 and 107.1 mm/month in the upper and middle reaches, respectively), which tended to lead to larger $\bar{\epsilon}_{TRMM}$. Nonetheless, $\bar{\epsilon}_{TRMM}$ for the two sub-basins was lower than 8% of the corresponding P_{OBS} , and therefore P_{TRMM} is considered to be reliable for application to the YRB at monthly and annual time steps.

Figure 4 and Table 3 show the relationships between ET_{MODIS} and the four GLDAS evapotranspiration datasets (monthly time steps) from 2003 to 2012. r , $\bar{\epsilon}_{MODIS}$ and $\bar{\epsilon}_{MODIS,b}$ were 0.99 ($P < 0.05$), 10.3 and -4.3 mm/month (i.e., MODIS data under-estimate GLDAS evapotranspiration), respectively, where ET_{MODIS} is compared to the

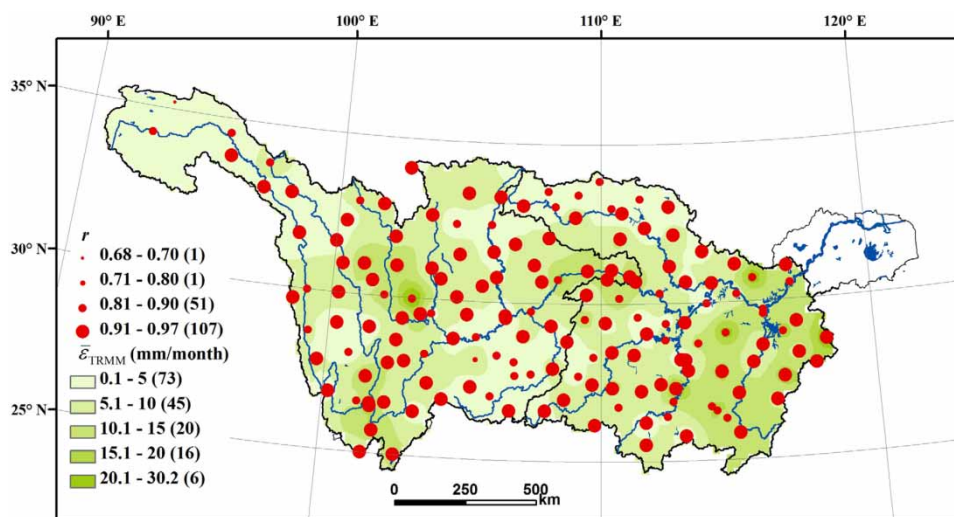


Figure 2 | Spatial distribution of the relationship between TRMM precipitation and observed precipitation from 2003 to 2012 for the YRB. The red dots are correlation coefficient r . Background colours represent TRMM precipitation error $\bar{\epsilon}_{TRMM}$, interpolated from 160 meteorological stations. The value in brackets is the number of stations out of 160 in the corresponding categories. Please refer to the online version of this paper to see this figure in colour: <http://dx.doi.org/10.2166/nh.2016.138>.

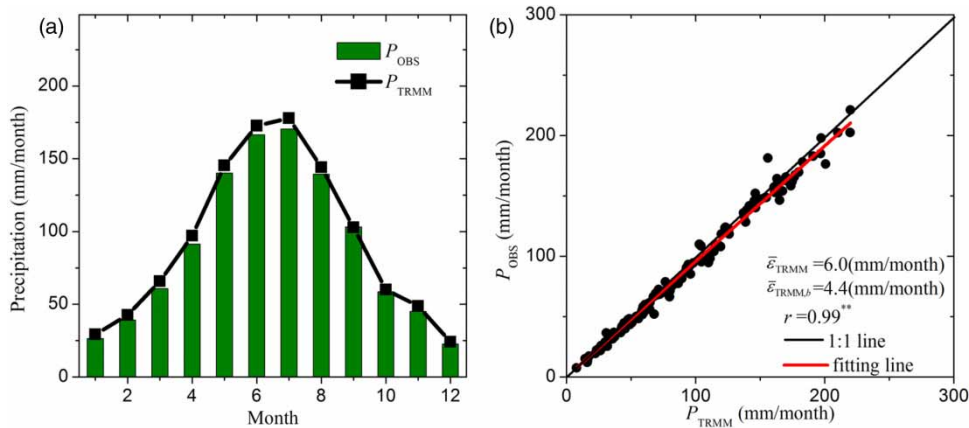


Figure 3 | (a) Monthly averages of TRMM precipitation and observed precipitation in the YRB for 2003–2012 and (b) scatter plot of monthly TRMM precipitation and observed precipitation from 2003 to 2012. ** indicates that the relationship is significant at the level of 0.05 by T-test.

Table 2 | Error statistics of satellite products in the YRB

Basin	Time steps	P_{Obs}	Error					
			$\bar{\epsilon}_{TRMM}$	$\bar{\epsilon}_{MODIS}^a$	$\bar{\epsilon}_{GRACE}^b$	$\bar{\epsilon}_Q$	$\bar{\epsilon}_{Q2}$	$\bar{\epsilon}$
YRB	Monthly (mm/month)	88.9	6.0	10.3	15.3	19.4	21.4	18.1
	Annual (mm/yr)	1066.2	54.3	51.9		76.7	141.2	152.5
Upper reaches of the YRB	Monthly (mm/month)	72.8	5.5	12.5	16.2	21.2	26.0	20.4
	Annual (mm/yr)	873.5	47.5	25.2		56.2	182.4	183.2
Middle reaches of the YRB	Monthly (mm/month)	107.1	8.0	9.5	24.1	27.1	25.5	20.5
	Annual (mm/yr)	1284.6	65.9	84.5		109.8	89.0	110.1

^aCalculated between ET_{MODIS} and the average values of the four GLDAS datasets.

^bEstimated by the GRACE measurement error and leakage error.

average of the four GLDAS datasets. At annual time steps, $\bar{\epsilon}_{MODIS}$ was 51.9 mm/yr for the YRB, which accounted for 5% of P_{OBS} (shown in Table 2). $\bar{\epsilon}_{MODIS}$ for the upper reaches of the YRB was smaller than that for the middle reaches of the YRB at the two time steps. In addition, r was 0.95 ($P < 0.05$) between the monthly ET_{MODIS} and ET_{OBS} from Qianyanzhou station although the observed time series was short (Figure 4(c)). $\bar{\epsilon}_{MODIS,b}$ shows that ET_{MODIS} was 13.5 mm/month larger than ET_{OBS} on average. $\bar{\epsilon}_{MODIS}$ was 14.3 mm/month, accounting for 16% of the YRB P_{OBS} .

The spatial distribution in $\bar{\epsilon}_{GRACE}$ is illustrated in Figure 5, which shows an error range of 18.1 to 145 mm/month, with most cells smaller than 70 mm/month. The basin average $\bar{\epsilon}_{GRACE}$ for the YRB, upper reaches and middle reaches were 15.3 mm/month, 16.2 mm/month and 24.1 mm/month, respectively. This highlights the smaller

errors that arise from averaging GRACE data over larger areas (Tapley *et al.* 2004; Horwath & Dietrich 2006).

Figure 6 shows the time series of ΔS_{GRACE} and ΔS_{WB} for 2003–2012, and the accompanying r values, which were 0.71 ($P < 0.05$), 0.77 ($P < 0.05$) and 0.56 ($P < 0.05$) for the YRB, upper and middle reaches, respectively. These results suggest reasonable correlations between ΔS_{GRACE} and ΔS_{WB} , albeit the peak of TWSC values, occurring during the wet season, are clearly underestimated by the water balance results relative to GRACE data. It is interesting that ΔS_{WB} changes preceded ΔS_{GRACE} by approximately one month for the middle reaches of the YRB (r between ΔS_{GRACE} and one-month lagged ΔS_{WB} was improved to 0.79, $P < 0.05$). This is likely caused in part by the calculation of Q_{OBS} in the water balance equation, as the stream flow difference between Datong and Yichang

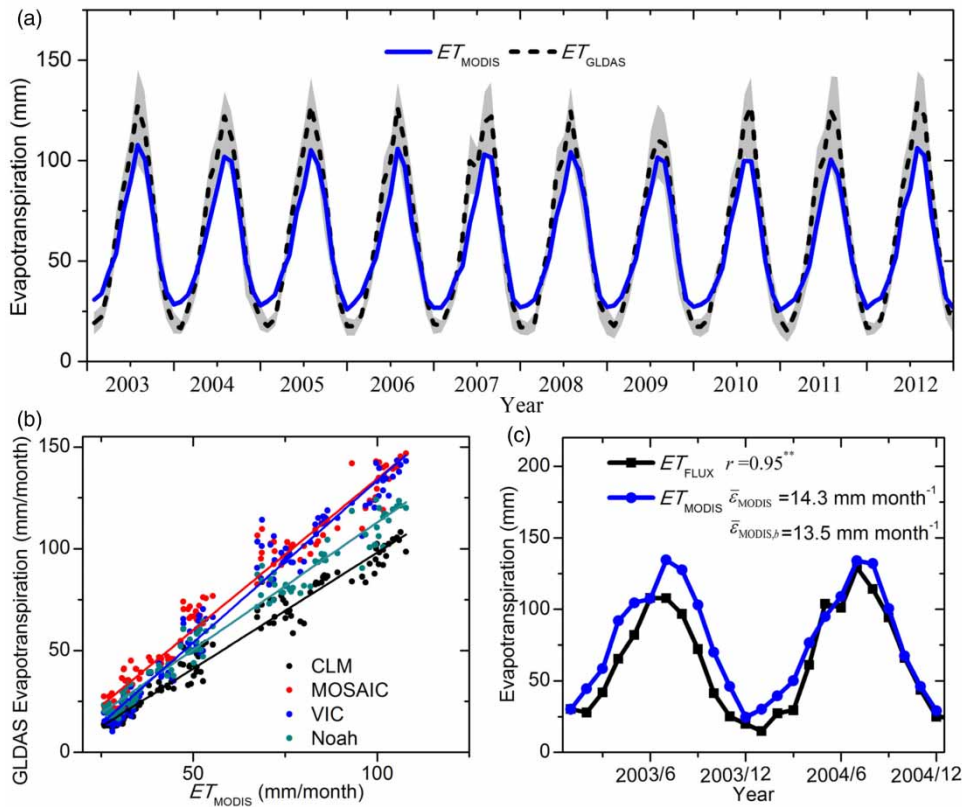


Figure 4 | (a) Time series of evapotranspiration datasets from MODIS and GLDAS for the YRB during 2003–2012 (the grey area represents the range of the four GLDAS evapotranspiration datasets and the black dashed line represents the GLDAS average); (b) relationship between ET_{MODIS} and the four datasets of GLDAS evapotranspiration; and (c) distribution of ET_{MODIS} and ground-based measurements of ET_{FLUX} during 2003–2004. ** indicates that the relationship is significant at the level of 0.05 by T-test.

Table 3 | Relationship between MODIS product and GLDAS evapotranspiration

Basin	Relationship	CLM	MOSAIC	VIC	Noah	Average
YRB	r	0.98**	0.98**	0.99**	0.98**	0.99**
	\bar{e}_{MODIS} (mm/month)	8.5	16.7	16.1	7.5	10.3
	$\bar{e}_{MODIS,b}$ (mm/month)	7.8	-14.0	-8.7	-2.4	-4.3
Upper reaches of the YRB	r	0.99**	0.98**	0.98**	0.98**	0.99**
	\bar{e}_{MODIS} (mm/month)	10.3	16.2	16.3	9.9	12.5
	$\bar{e}_{MODIS,b}$ (mm/month)	6.2	-10.1	-4.7	0.2	-2.1
Middle reaches of the YRB	r	0.97**	0.97**	0.98**	0.97**	0.98**
	\bar{e}_{MODIS} (mm/month)	11.2	19.8	17.5	9.0	9.5
	$\bar{e}_{MODIS,b}$ (mm/month)	10.4	-18.7	-13.5	-6.3	-7.0

**Indicates that the relationship is significant at the level of 0.05 by T-test.

stations. These stations are about 900 km apart, and therefore, the significant time lag associated with Yangtze River flood waves will create stream flow differences at the two stations that are not necessarily a product of runoff from the middle reaches.

Water balance errors by satellite products

Among the three satellite products, the error of GRACE TWSC was the largest at monthly time steps, followed by MODIS evapotranspiration and TRMM precipitation (see

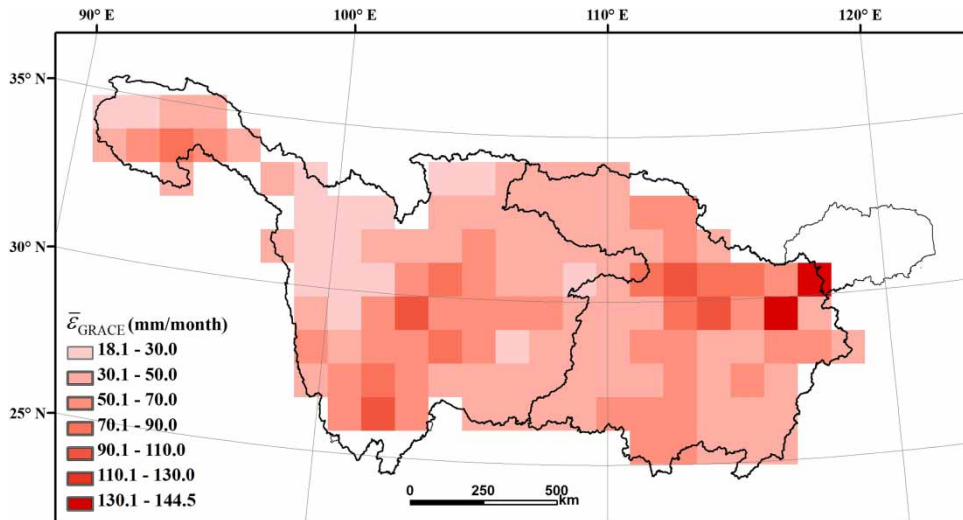


Figure 5 | Spatial distribution of GRACE TWS error for the YRB.

Table 2), while TRMM precipitation had the largest error at annual time steps, followed by MODIS evapotranspiration and GRACE TWSC. It should be noted that GRACE TWSC error is influenced by measurement error and leakage error (the residual errors after filtering and rescaling), because there are no observed TWSC data that cover a reasonable proportion of the respective basins. TRMM and MODIS errors were obtained by comparing directly to ground-based and model-based values, and as such, are not subjected to the same uncertainties as the calculations of GRACE errors. Nevertheless, the error estimation method used in this study offers useful insights into discrepancies in the satellite-based water balance components.

The error in stream flow ($\bar{\epsilon}_Q$) arising from combining water budget components from satellite products was 19.4 mm/month and 76.7 mm/yr for the YRB at monthly and annual time steps accounting for 22% and 7% of YRB P_{OBS} , respectively. Table 2 shows that $\bar{\epsilon}_Q$ for the upper reaches of the YRB was smaller than that of the middle reaches of the YRB, at both monthly and annual time steps. In addition, the estimated stream flow was compared with observed values. $\bar{\epsilon}_{Q2}$ for the YRB was 21.4 mm/month and 141.2 mm/yr at monthly and annual time steps and both were larger than $\bar{\epsilon}_Q$. $\bar{\epsilon}_{Q2}$ for the upper reaches of the YRB was larger than that for the middle reaches of the YRB. The discrepancies between $\bar{\epsilon}_Q$ and $\bar{\epsilon}_{Q2}$ reflect nonlinearities in the errors in stream flow obtained from the summation

of satellite products that detract from the reliability of Equation (6).

Water balance errors ($\bar{\epsilon}$) obtained using Equation (4) are shown in Table 2. $\bar{\epsilon}$ for the YRB was 18.1 mm/month and 152.5 mm/yr at monthly and annual time steps, accounting for 20% and 14% of YRB P_{OBS} , respectively. $\bar{\epsilon}$ values for the upper and middle sub-basins were similar at monthly time steps, accounting for 28% and 19% of YRB P_{OBS} , respectively. However, $\bar{\epsilon}$ for the upper reaches of the YRB was much larger than that for the middle reaches of the YRB at annual time steps, accounting for 21% and 9% of corresponding P_{OBS} , respectively. The reason was the larger overestimated TRMM precipitation and underestimated MODIS evapotranspiration in the middle reaches of the YRB than that in the upper reaches.

Changes in water balance components

Table 4 shows the relationships between trends in satellite products and ground-based/model-based datasets for the YRB at monthly time steps. The only clear relationships were obtained for precipitation. This suggests that monthly time series of MODIS, GRACE and estimated stream flow were not suitable for identifying temporal trends in these components of the YRB water balance, despite there being good correlations in the absolute values. Table 5 shows the comparison of water balance component trends using annual time series. For the entire YRB, the rates of changes

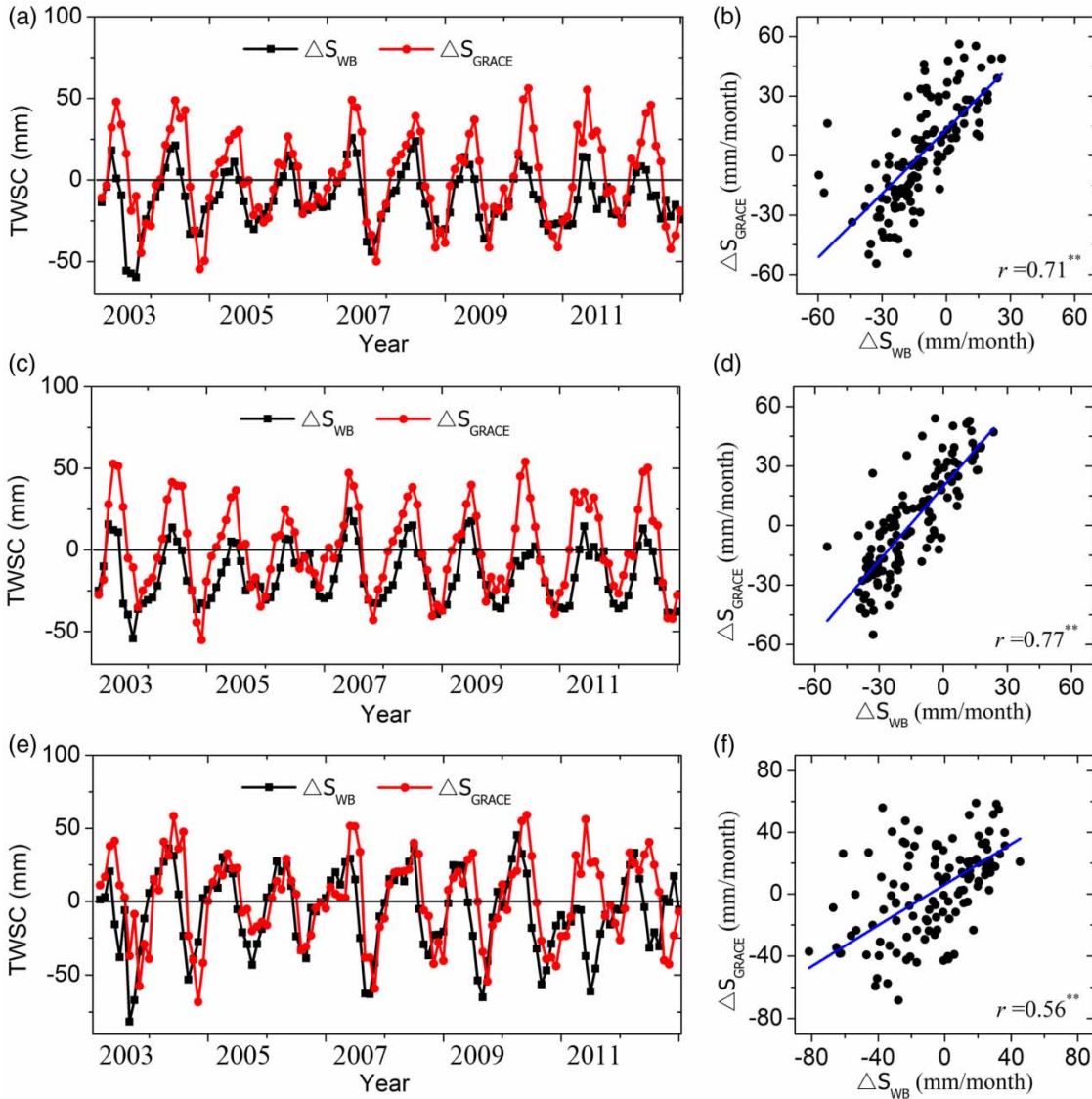


Figure 6 | (a) Time series of TWSC by GRACE product and water balance method and (b) the relationship between the two TWSC for the YRB. (c)–(d) and (e)–(f) represent the same as (a)–(b), but for the upper and middle reaches of the YRB, respectively. **indicates relationship is significant at the level of 0.05 by T-test.

Table 4 | Correlation coefficient between trends in satellite products and ground-based/model-based datasets at monthly time steps

Basin	P_{TRMM} vs. P_{OBS}	ET_{MODIS} vs. ET_{GLDAS}	ΔS_{GRACE} vs. ΔS_{WB}	Q_{RS} vs. Q_{OBS}
YRB	0.84**	0.60**	0.35	-0.07
Upper reaches of the YRB	0.80**	-0.15	-0.34	-0.11
Middle reaches of the YRB	0.90**	0.43	0.51**	0.31

^aCalculated by the average values of the four GLDAS datasets.

**Indicates that relationship is significant at the level of 0.05 by T-test.

in P_{TRMM} , ET_{MODIS} , ΔS_{GRACE} and Q_{RS} are 173%, 318%, 240% and 83%, respectively, of corresponding ground-based/model-based slope. Although the rates of changes in satellite-based water balance components for the upper reaches of the YRB are extremely large due to the slight trends in Q_{OBS} and ET_{GLDAS} , the rates of changes in satellite-based water balance components for the middle reaches of the YRB are within 129–170%. Generally, the satellite products are more suitable for studying the trends in annual time series compared with monthly time series.

Table 5 | Trends in water balance components based on satellite products in the YRB from 2003 to 2012 (mm/yr²)

Basin	P_{TRMM}	P_{Obs}	ET_{MODIS}	ET_{GLDAS}^a	ΔS_{GRACE}	ΔS_{WB}	Q_{RS}	Q_{Obs}
YRB	6.9	4.0	-3.5**	-1.1	7.2*	3.0	1.9	2.3
Upper reaches of the YRB	-1.4	-3.7	-3.1	0.4	5.3*	2.3	-2.9	0.1
Middle reaches of the YRB	16.4	12.7	-4.2**	-3.0	9.7	5.7	8.8	5.5

^aCalculated by the average values of the four GLDAS datasets.

*Indicates that slope is significant at the level of 0.01 by T-test.

**Indicates that slope is significant at the level of 0.05 by T-test.

Figure 7 illustrates the spatial distributions of trends (determined from annual time series) in satellite-based water balance components. During the period 2003–2012, the slope of P_{TRMM} ranged from -55.9 to 97.7 mm/yr² (Figure 7(a)). P_{TRMM} in the upper reaches of the YRB decreased slightly at -1.4 mm/yr², while P_{TRMM} in the middle reaches of the YRB increased at 16.4 mm/yr². For the entire YRB, P_{TRMM} increased at 6.9 mm/yr² from 2003 to 2010.

ET_{MODIS} changed at rates ranging from -76.6 to 55.4 mm/yr² (Figure 7(b)) at annual time steps. ET_{MODIS} for the middle reaches decreased significantly ($P < 0.05$) at a rate of -4.2 mm/yr², while there was no significant trend in ET_{MODIS} in the upper reaches. For the entire YRB, ET_{MODIS} decreased significantly ($P < 0.05$) at a rate of -3.5 mm/yr². The decrease in evapotranspiration was a complex result of decreases in air temperature, wind speed, vapor pressure and solar radiation (Figure 8), as reported by Roderick & Farquhar (2002), Liu *et al.* (2011) and Zhang *et al.* (2015).

Figure 7(c) shows the spatial distribution of ΔS_{GRACE} trends, which ranged from -1.9 to 28.9 mm/yr². For the entire YRB, ΔS_{GRACE} increased significantly ($P < 0.1$) at a rate of 7.2 mm/yr². The increasing trend in ΔS_{GRACE} for the middle reaches of the YRB was about 1.8 times that for the upper reaches of the YRB. The increased precipitation and decreased evapotranspiration, in combination, resulted in increased ΔS_{GRACE} , especially for the middle reaches of the YRB. In addition, the forest cover increased markedly under soil and water conservation policies (Gao *et al.* 2014; Zhang *et al.* 2015), which likely also modified the basin's soil water storage capacity, and thereby affected the TWSC of the YRB.

The slope of Q_{RS} (Figure 7(d)), based on the residual of TRMM, MODIS and GRACE results, was between -35.4 and 94.7 mm/yr². Q_{RS} decreased for the upper reaches of the YRB at a rate of -2.9 mm/yr², while it increased for

the middle reaches of the YRB at a rate of 8.8 mm/yr². For the entire YRB, the rate of changes in Q_{RS} was 1.9 mm/yr². Table 2 indicates a somewhat reasonable consistency between stream flow estimated from satellite products and ground-based measurements, at least at annual time steps.

It is difficult to provide definitive explanation of the causes of changes in water balance components, and discrepancies between satellite- and ground-based estimates of trends, because water balance trends are interdependent. For example, decreasing trends in precipitation are expected to produce reducing stream flow, evaporation variations influence the regional climate and subsequently modify the regional precipitation, and water storage changes modify evaporation and stream flow, etc. (Kumagai *et al.* 2013). In addition, the operation of TGD may have modified several water cycle components of the YRB (Li *et al.* 2013a, 2013b; Lai *et al.* 2014; Zhang *et al.* 2014). TGD impounds water from September to October, and releases water from March to June. If TGD impacts the water cycle of the YRB, the relationships between the upper (considered as the unaffected region of TGD) and middle reaches (considered as the TGD-affected region) of the YRB would be disrupted during the impoundment and release periods. Figure 9 shows the correlations of ΔS_{GRACE} between the upper and middle reaches. There were good relationships of ΔS_{GRACE} between the two sub-basins during the impoundment and release periods, which indicates TGD has limited impact on YRB's ΔS_{GRACE} . This is consistent with the result of Li *et al.* (2013a, 2013b), who concluded that the hydrological drought at the downstream Yichang station was slightly aggravated by TGD's operation from 2003 to 2011.

It is important to highlight some of the main uncertainties in the results of this study. For example, given the lack of actual evapotranspiration observations, ET_{MODIS} was compared with evapotranspiration by GLDAS to evaluate the

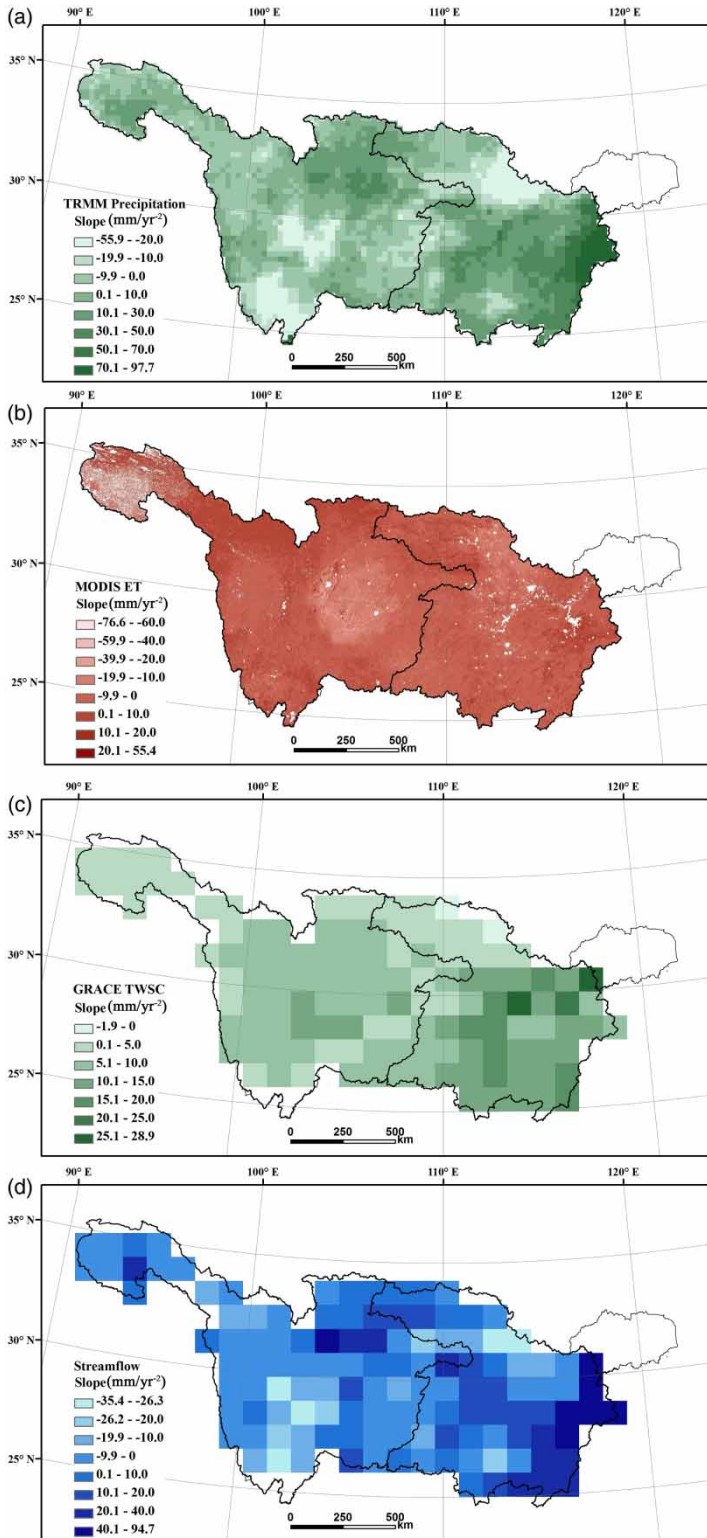


Figure 7 | Spatial distributions of trends in water balance components from 2003 to 2012 for the YRB: (a) TRMM precipitation; (b) MODIS evapotranspiration; (c) GRACE TWSC; and (d) stream flow as the sum of multiple satellite products.

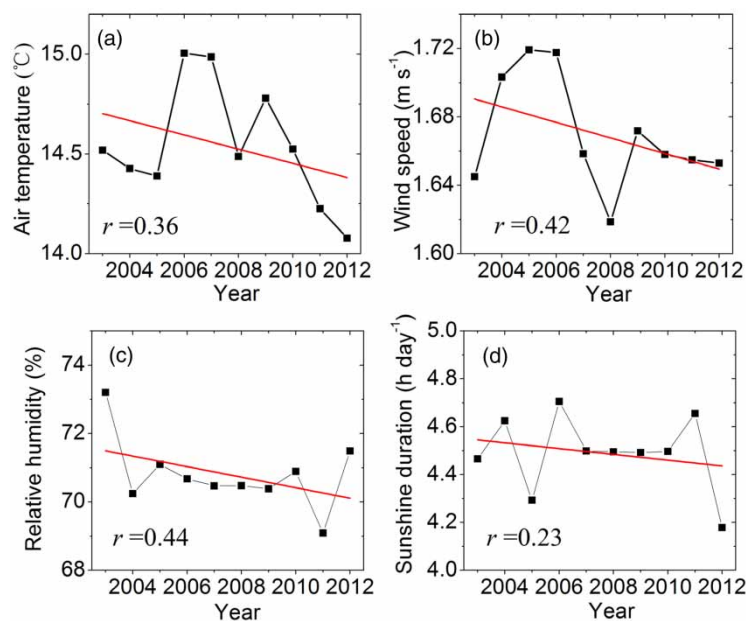


Figure 8 | Variations in (a) air temperature, (b) wind speed, (c) relative humidity and (d) sunshine duration from 2003 to 2012 for the YRB.

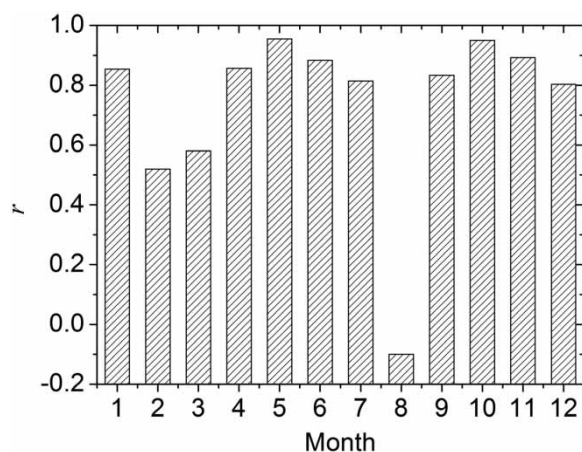


Figure 9 | Relationships of GRACE TWSC between the upper reaches of the YRB and the middle reaches of the YRB during 2003–2012.

errors in ET_{MODIS} . While employing different measurements to quantify errors in remotely sensed water balance components will impart some inequity in the evaluation of sources of error, there are limited alternatives to the evaluation of water balance errors at the scale of the study area. In addition, the resolutions of satellite products are different, and the different re-sampling methods will influence the resulting Q_{RS} values (Wald *et al.* 1997). The different spatial resolutions of satellite products used in this study required

re-sampling at the coarsest resolution among the three products (1°) to estimate Q_{RS} .

In agreement with previous studies (e.g., Sahoo *et al.* 2011; Armanios & Fisher 2014; Oliveira *et al.* 2014), the absolute values of the water balance components are found to be consistent with ground-based/model-based time series. As an extension to earlier investigations, this study demonstrated that there are weak relationships between trends (from monthly time series) in water balance components by satellite products and ground-based/model-based sources, whereas reasonable consistency was obtained in the trends of annual time series.

CONCLUSIONS

This study evaluated the water balance of the YRB from 2003 to 2012 by the following three satellite products: TRMM precipitation, MODIS evapotranspiration and GRACE TWSC, and the changes in water balance components were analyzed. TRMM and MODIS products performed well in reproducing monthly precipitation and evapotranspiration obtained from ground-based observation and land surface model datasets, respectively. A good relationship between GRACE TWSC and the residual water storage from a water balance equation was identified (correlation coefficient of 0.71). The water

balance error for the YRB was 18.1 mm/month and 152.5 mm/yr at monthly and annual time steps, accounting for 20% and 14% of YRB precipitation, respectively. The error in GRACE TWS was the largest among the three satellite products at monthly time steps, while the error in TRMM precipitation was the largest at annual time steps. The temporal changes in water balance components based on satellite products performed better at an annual time step compared to a monthly time step. Rates of change in the water balance components for the YRB at annual time steps were in the range 83–318% of the corresponding trends from ground-based and model-based datasets. The estimated stream flow by satellite products for the YRB increased at a rate of 1.9 mm/yr² during 2003–2012, which was consistent with ground-based stream flow changes (the slope of 2.3 mm/yr²).

This study evaluated the reliability of multiple satellite products used in a water balance equation, and found that the three products were more suitable for water cycle investigation at annual, rather than monthly, time steps. The current investigation is an improvement on previous studies that assess the accuracy of basin-scale hydrological components separately. This study demonstrates that water balance investigation using remote sensing products is a practical and informative undertaking that is expected to continue to evolve with refinements to inversion algorithms and the spatial and temporal resolution of datasets.

ACKNOWLEDGEMENTS

This research was supported by the National Basic Research Program of China (2012CB417003), Natural Science Foundation of China (41330529, 41401032 and 41371062), Natural Sciences Foundation of Jiangsu Province (BK20141059) and Open Foundation of State Key Laboratory of Hydrology-Water Resources and Hydraulic Engineering (2014490811).

REFERENCES

Adjei, K. A., Ren, L., Appiah-Adjei, E. K. & Odai, S. N. 2014 Application of satellite-derived rainfall for hydrological

- modelling in the data-scarce Black Volta trans-boundary basin. *Hydrol. Res.* **46**, 777–791.
- Al-Mukhtar, M., Dunger, V. & Merkel, B. 2014 Evaluation of the climate generator model CLIGEN for rainfall data simulation in Bautzen catchment area, Germany. *Hydrol. Res.* **45**, 615–630.
- Armanios, D. E. & Fisher, J. B. 2014 Measuring water availability with limited ground data: assessing the feasibility of an entirely remote-sensing-based hydrologic budget of the Rufiji Basin, Tanzania, using TRMM, GRACE, MODIS, SRB, and AIRS. *Hydrol. Processes* **28**, 853–867.
- Barros, A., Joshi, M., Putkonen, J. & Burbank, D. 2000 A study of the 1999 monsoon rainfall in a mountainous region in central Nepal using TRMM products and rain gauge observations. *Geophys. Res. Lett.* **27**, 3683–3686.
- Benz, U. C., Hofmann, P., Willhauck, G., Lingenfelder, I. & Heynen, M. 2004 Multi-resolution, object-oriented fuzzy analysis of remote sensing data for GIS-ready information. *Isprs J. Photogramm.* **58**, 239–258.
- Cai, X., Yang, Z. L., Xia, Y., Huang, M., Wei, H., Leung, L. R. & Ek, M. B. 2014 Assessment of simulated water balance from Noah, Noah-MP, CLM, and VIC over CONUS using the NLDAS test bed. *J. Geophys. Res.* **119**, 13751–13770.
- Castro, L. M., Salas, M. M. & Fernández, B. 2015 Evaluation of TRMM multi-satellite precipitation analysis (TMPA) in a mountainous region of the central Andes range with a Mediterranean climate. *Hydrol. Res.* **46**, 89–105.
- Corbari, C., Mancini, M., Su, Z. & Li, J. 2014 Evapotranspiration estimate from water balance closure using satellite data for the Upper Yangtze River basin. *Hydrol. Res.* **45**, 603–614.
- Dai, Z., Du, J., Li, J., Li, W. & Chen, J. 2008 Runoff characteristics of the Changjiang River during 2006: effect of extreme drought and the impounding of the Three Gorges Dam. *Geophys. Res. Lett.* **35**, L07406. doi:10.1029/2008GL033456.
- Finsen, F., Milzow, C., Smith, R., Berry, P. & Bauer-Gottwein, P. 2014 Using radar altimetry to update a large-scale hydrological model of the Brahmaputra river basin. *Hydrol. Res.* **45**, 148–164.
- Gao, G., Ding, G., Zhao, Y., Bao, Y. & Yu, M. 2014 Forestry solutions for mitigating climate change in China. *For. Syst.* **23**, 183–186.
- Guo, H., Hu, Q., Zhang, Q. & Feng, S. 2012 Effects of the Three Gorges Dam on Yangtze river flow and river interaction with Poyang Lake, China: 2003–2008. *J. Hydrol.* **416**, 19–27.
- He, T. & Shao, Q. 2014 Spatial-temporal variation of terrestrial evapotranspiration in China from 2001 to 2010 using MOD16 Products. *J. Geo-information Sci.* **16**, 979–987.
- Horwath, M. & Dietrich, R. 2006 Errors of regional mass variations inferred from GRACE monthly solutions. *Geophys. Res. Lett.* **33**, L07502. doi:10.1029/2005GL025550.
- Houser, P. R., Rodell, M., Jambor, U., Gottschalck, J., Cosgrove, B., Radakovich, J., Arsenault, K., Bosilovich, M., Entin, J. & Walker, J. 2001 The global land data assimilation system. *GEWEX News* **11**, 11–13.

- Huang, Q., Sun, Z., Opp, C., Lotz, T., Jiang, J. & Lai, X. 2014 Hydrological Drought at Dongting Lake: its detection, characterization, and challenges associated with Three Gorges Dam in Central Yangtze, China. *Water Resour. Manag.* **28**, 5377–5388.
- Huffman, G. J., Bolvin, D. T., Nelkin, E. J., Wolff, D. B., Adler, R. F., Gu, G., Hong, Y., Bowman, K. P. & Stocker, E. F. 2007 The TRMM multisatellite precipitation analysis (TMPA): Quasi-global, multiyear, combined-sensor precipitation estimates at fine scales. *J. Hydrometeorol.* **8**, 38–55.
- Kang, K. & Merwade, V. 2014 The effect of spatially uniform and non-uniform precipitation bias correction methods on improving NEXRAD rainfall accuracy for distributed hydrologic modeling. *Hydrol. Res.* **45**, 23–42.
- Kim, H. W., Hwang, K., Mu, Q., Lee, S. O. & Choi, M. 2012 Validation of MODIS 16 global terrestrial evapotranspiration products in various climates and land cover types in Asia. *KSCE J. Civ. Eng.* **16**, 229–238.
- Kumagai, T. O., Kanamori, H. & Yasunari, T. 2013 Deforestation-induced reduction in rainfall. *Hydrol. Processes* **27**, 3811–3814.
- Kummerow, C., Barnes, W., Kozu, T., Shiue, J. & Simpson, J. 1998 The tropical rainfall measuring mission (TRMM) sensor package. *J. Atmos. Ocean. Tech.* **15**, 809–817.
- Lai, X., Jiang, J., Yang, G. & Lu, X. 2014 Should the Three Gorges Dam be blamed for the extremely low water levels in the middle-lower Yangtze River? *Hydrol. Processes* **28**, 150–160.
- Lakshmi, V., Hong, S., Small, E. E. & Chen, F. 2011 The influence of the land surface on hydrometeorology and ecology: new advances from modeling and satellite remote sensing. *Hydrol. Res.* **42**, 95–112.
- Landerer, F. & Swenson, S. 2012 Accuracy of scaled GRACE terrestrial water storage estimates. *Water Resour. Res.* **48**, W04531. doi:10.1029/2011WR011453.
- Li, X., Zhang, Q. & Xu, C. Y. 2012 Suitability of the TRMM satellite rainfalls in driving a distributed hydrological model for water balance computations in Xinjiang catchment, Poyang lake basin. *J. Hydrol.* **426**, 28–38.
- Li, L., Ngongondo, C. S., Xu, C. Y. & Gong, L. 2013a Comparison of the global TRMM and WFD precipitation datasets in driving a large-scale hydrological model in Southern Africa. *Hydrol. Res.* **5**, 770–778.
- Li, S., Xiong, L., Dong, L. & Zhang, J. 2013b Effects of the Three Gorges Reservoir on the hydrological droughts at the downstream Yichang station during 2003–2011. *Hydrol. Processes* **27**, 3981–3993.
- Li, Z., Yang, D., Gao, B., Jiao, Y., Hong, Y. & Xu, T. 2014 Multi-scale hydrologic applications of the latest satellite precipitation products in the Yangtze River Basin using a distributed hydrologic model. *J. Hydrometeorol.* **16**, 407–426.
- Liu, X., Luo, Y., Zhang, D., Zhang, M. & Liu, C. 2011 Recent changes in pan-evaporation dynamics in China. *Geophys. Res. Lett.* **38**, L13404. doi:10.1029/2011GL047929.
- Long, D., Longuevergne, L. & Scanlon, B. R. 2014 Uncertainty in evapotranspiration from land surface modeling, remote sensing, and GRACE satellites. *Water Resour. Res.* **50**, 1131–1151.
- Maidment, D. R. 1992 *Handbook of Hydrology*. McGraw-Hill Inc., New York.
- Moiwo, J. P., Tao, F. & Lu, W. 2013 Analysis of satellite-based and in situ hydro-climatic data depicts water storage depletion in North China Region. *Hydrol. Processes* **27**, 1011–1020.
- Mu, Q., Zhao, M. & Running, S. W. 2011 Improvements to a MODIS global terrestrial evapotranspiration algorithm. *Remote Sens. Environ.* **115**, 1781–1800.
- Oliveira, P. T. S., Nearing, M. A., Moran, M. S., Goodrich, D. C., Wendland, E. & Gupta, H. V. 2014 Trends in water balance components across the Brazilian Cerrado. *Water Resour. Res.* **50**, 7100–7114.
- Peters-Lidard, C. D., Kumar, S. V., Mocko, D. M. & Tian, Y. 2011 Estimating evapotranspiration with land data assimilation systems. *Hydrol. Processes* **25**, 3979–3992.
- Pohl, C. & van Genderen, J. L. 1998 Review article multisensor image fusion in remote sensing: concepts, methods and applications. *Int. J. Remote Sens.* **19**, 823–854.
- Reager, J. & Famiglietti, J. S. 2013 Characteristic mega-basin water storage behavior using GRACE. *Water Resour. Res.* **49**, 3314–3329.
- Reichle, R. H., Koster, R. D., Dong, J. & Berg, A. A. 2004 Global soil moisture from satellite observations, land surface models, and ground data: implications for data assimilation. *J. Hydrometeorol.* **5**, 430–442.
- Rodell, M., Famiglietti, J., Chen, J., Seneviratne, S., Viterbo, P., Holl, S. & Wilson, C. 2004 Basin scale estimates of evapotranspiration using GRACE and other observations. *Geophys. Res. Lett.* **31**, L20504. doi:10.1029/2004GL020873.
- Roderick, M. L. & Farquhar, G. D. 2002 The cause of decreased pan evaporation over the past 50 years. *Science* **298**, 1410–1411.
- Sahoo, A. K., Pan, M., Troy, T. J., Vinukollu, R. K., Sheffield, J. & Wood, E. F. 2011 Reconciling the global terrestrial water budget using satellite remote sensing. *Remote Sens. Environ.* **115**, 1850–1865.
- Scheel, M. L. M., Rohrer, M., Huggel, C., Santos Villar, D., Silvestre, E. & Huffman, G. J. 2011 Evaluation of TRMM Multi-satellite Precipitation Analysis (TMPA) performance in the Central Andes region and its dependency on spatial and temporal resolution. *Hydrol. Earth. Syst. Sci.* **15**, 2649–2663.
- Sheffield, J., Ferguson, C. R., Troy, T. J., Wood, E. F. & McCabe, M. F. 2009 Closing the terrestrial water budget from satellite remote sensing. *Geophys. Res. Lett.* **36**, L07403. doi:10.1029/2009GL037338.
- Su, F., Hong, Y. & Lettenmaier, D. P. 2008 Evaluation of TRMM multisatellite precipitation analysis (TMPA) and its utility in hydrologic prediction in the La Plata Basin. *J. Hydrometeorol.* **9**, 622–640.
- Sun, Z., Wang, Q., Ouyang, Z., Watanabe, M., Matsushita, B. & Fukushima, T. 2007 Evaluation of MOD16 algorithm using MODIS and ground observational data in winter wheat field in North China Plain. *Hydrol. Processes* **21**, 1196–1206.

- Sun, S., Chen, H., Ju, W., Yu, M., Hua, W. & Yin, Y. 2014 On the attribution of the changing hydrological cycle in Poyang Lake Basin, China. *J. Hydrol.* **514**, 214–225.
- Swenson, S. & Wahr, J. 2009 Monitoring the water balance of Lake Victoria, East Africa, from space. *J. Hydrol.* **370**, 163–176.
- Tang, J., Cheng, H. & Liu, L. 2014 Assessing the recent droughts in Southwestern China using satellite gravimetry. *Water Resour. Res.* **50**, 3030–3038.
- Tapley, B. D., Bettadpur, S., Ries, J. C., Thompson, P. F. & Watkins, M. M. 2004 GRACE measurements of mass variability in the earth system. *Science* **305**, 503–505.
- Varis, O. & Vakkilainen, P. 2001 China's 8 challenges to water resources management in the first quarter of the 21st Century. *Geomorphol.* **41**, 93–104.
- Venturini, V., Islam, S. & Rodriguez, L. 2008 Estimation of evaporative fraction and evapotranspiration from MODIS products using a complementary based model. *Remote Sens. Environ.* **112**, 132–141.
- Wald, L., Ranchin, T. & Mangolini, M. 1997 Fusion of satellite images of different spatial resolutions: assessing the quality of resulting images. *Photogramm. Eng. Remote Sens.* **63**, 691–699.
- Wang, K. & Dickinson, R. E. 2012 A review of global terrestrial evapotranspiration: observation, modeling, climatology, and climatic variability. *Rev. Geophys.* **50**, 1–54.
- Wang, H., Guan, H., Gutiérrez-Jurado, H. A. & Simmons, C. T. 2014a Examination of water budget using satellite products over Australia. *J. Hydrol.* **511**, 546–554.
- Wang, S., Huang, J., Li, J., Rivera, A., McKenney, D. W. & Sheffield, J. 2014b Assessment of water budget for sixteen large drainage basins in Canada. *J. Hydrol.* **512**, 1–15.
- Wilson, K. B., Hanson, P. J., Mulholland, P. J., Baldocchi, D. D. & Wullschleger, S. D. 2001 A comparison of methods for determining forest evapotranspiration and its components: sap-flow, soil water budget, eddy covariance and catchment water balance. *Agr. For. Meteorol.* **106**, 153–168.
- Wolff, D. B., Marks, D., Amitai, E., Silberstein, D., Fisher, B., Tokay, A., Wang, J. & Pippitt, J. 2005 Ground validation for the tropical rainfall measuring mission (TRMM). *J. Atmos. Ocean. Tech.* **22**, 365–380.
- Wu, S.-J., Lien, H.-C., Hsu, C.-T., Chang, C.-H. & Shen, J.-C. 2015 Modeling probabilistic radar rainfall estimation at ungauged locations based on spatiotemporal errors which correspond to gauged data. *Hydrol. Res.* **46**, 39–59.
- Xu, H., Xu, C.-Y., Sælthun, N. R., Zhou, B. & Xu, Y. 2015 Evaluation of reanalysis and satellite-based precipitation datasets in driving hydrological models in a humid region of Southern China. *Stoch. Env. Res. Risk. A.* **29**, 2003–2020.
- Yang, S. & Nesbitt, S. W. 2014 Statistical properties of precipitation as observed by the TRMM precipitation radar. *Geophys. Res. Lett.* **41**, 5636–5643.
- Zhang, Q., Ye, X., Werner, A. D., Li, Y., Yao, J., Li, X. & Xu, C. 2014 An investigation of enhanced recessions in Poyang Lake: comparison of Yangtze River and local catchment impacts. *J. Hydrol.* **517**, 425–434.
- Zhang, D., Hong, H., Zhang, Q. & Li, X. 2015 Attribution of the changes in annual streamflow in the Yangtze River Basin over the past 146 years. *Theor. Appl. Climatol.* **119**, 323–332.
- Zhao, H., Yang, S., Wang, Z., Zhou, X., Luo, Y. & Wu, L. 2015 Evaluating the suitability of TRMM satellite rainfall data for hydrological simulation using a distributed hydrological model in the Weihe River catchment in China. *J. Geogr. Sci.* **25**, 177–195.

First received 4 July 2015; accepted in revised form 17 November 2015. Available online 27 January 2016